IEEE Access
Multidisciplinary | Rapid Review | Open Access Journal

Received July 14, 2020, accepted August 8, 2020, date of publication August 14, 2020, date of current version August 25, 2020.

Digital Object Identifier 10.1109/ACCESS.2020.3016650

Adaptive Second-Order Sliding Mode Algorithm-Based Modified Function Projective Synchronization of Uncertain Hyperchaotic Systems

XUAN-TOA TRAN[1,2], CHEOLHYEON KWON[1], (Member, IEEE), AND HYONDONG OH[1], (Senior Member, IEEE)

[1]School of Mechanical, Aerospace and Nuclear Engineering, Ulsan National Institute of Science and Technology, Ulsan 44919, South Korea
[2]NTT Hi-Tech Institute, Nguyen Tat Thanh University, Ho Chi Minh City 70000, Vietnam

Corresponding authors: Cheolhyeon Kwon (kwon@unist.ac.kr) and Hyondong Oh (h.oh@unist.ac.kr)

This work was supported in part by the High-Assurance Cyber-Physical System from the Control Theoretic Perspective Research Fund of the Ulsan National Institute of Science and Technology (UNIST) under Grant 1.190140.01, and in part by the Basic Science Research Program through the National Research Foundation of Korea (NRF) funded by the Ministry of Education under Grant 2020R1A6A1A03040570.

ABSTRACT This article proposes a synchronization technique for uncertain hyperchaotic systems in the modified function projective manner using integral fast terminal sliding mode (I-FTSM) and adaptive second-order sliding mode algorithm. The new I-FTSM manifolds are introduced with the aim of having the fast convergence speed. The proposed continuous controller not only results in the robustness and high-accuracy synchronization in the presence of unknown external disturbances and/or model uncertainties but also helps alleviating the chattering effect significantly. Numerical simulation results are provided to illustrate the effectiveness of the proposed control design technique and verify the theoretical analysis.

INDEX TERMS Hyperchaotic synchronization, terminal sliding mode control, uncertainty, finite-time control.

I. INTRODUCTION

Synchronization of chaotic or hyperchaotic systems (HPSs) has attracted enormous research efforts from the control community as the recent reports have shown the potential in many areas such as secure communications, image encryption, information processing, diagnosis and identification, power converters, chemical reaction and biological systems [1]–[6]. In recent years, the modified function projective synchronization (MFPS) problem has gained a particular attention as it helps to address a more general type of synchronization [7]. Specifically, the MFPS is well-suited to secure communication and image encryption since the MFPS means that the states of the slave system are driven to follow those of the master system up to nonlinear smooth scaling functions that seem to be difficult to be predicted, thus substantially improving the signal encryption [4]–[6].

To achieve the MFPS, some control methods have been reported such as the Open-Plus-Closed-Loop coupling method [8], linear dynamic coupling [9], and reservoir computing scheme [10]. However, these schemes are not applicable for the HPSs that are perturbed by external disturbances and uncertainties (EDaU). Based on the Linear Matrix Inequality technique and Lyapunov stability theory, Mobayen and Tchier proposed new nonlinear control methods that could be extended to perform the MFPS in presence of EDaU assuming their upper bounds to be known a priori [11], [12]. However, it may not be easy to estimate the upper bounds of such perturbations. In order to overcome such challenges, adaptive control-based techniques have been proposed to obtain the MFPS against unknown perturbations [13]–[17]. Nevertheless, these methods only lead to synchronization with limited capabilities, *i.e.*, the MFPS errors are either bounded or converging to zero asymptotically.

Certainly, steering the synchronization error to zero within a finite time is more desirable, and finite-time MFPS (FT-MFPS) could be achieved by finite-time control (FTC)

The associate editor coordinating the review of this manuscript and approving it for publication was Zhongyang Fei.

methods. The fast convergence, high accuracy, robustness, and disturbance rejection ability are the demonstrated characteristics of the FTC [18]. Therefore, the FTC technique-based synchronization has been received an increasing attention in recent years [19]–[25]. Although only few FTC works are partially considering some sub-classes of MFPS in the current literature, they can be readily applied to a general MFPS problem after relevant modification. In [19], an adaptive FTC method is proposed to aim at finite-time synchronization (FTSY) of chaotic systems, where $tanh(\cdot)$ function was utilized to avoid the chattering effect. Sangpet and Kuntanapreeda [20] solved the FTSY problem by proposing a passivity-based feedback controller. Aghababa and his colleague in [21] addressed the adaptive FTSY of the uncertain non-autonomous chaotic system. The combination-combination synchronization of four different uncertain chaotic systems in finite time was studied in [22]. The authors in [23] introduced a new robust adaptive synchronization approach of hyperchaotic Rossler systems with unknown parameters based on FTC and back-stepping control. However, all the aforementioned studies contain inevitable drawbacks such as the requirement of the upper bound of uncertainty terms, unknown or estimated parameters are known a priori (see [21] and [22]); and the work in [23] is limited to the specific type of HPSs. Wang *et al.* [24] introduced an adaptive FTC for synchronizing uncertain Lorenz-Stenflo systems; however, their results only ensure the finite-time stability with special initial conditions related to the Lyapunov function candidate, which is hardly satisfied. On the basis of the finite-time stability theory, Zhang *et al.* [25] proposed a modified adaptive FTC strategy aimed at achieving the global FTSY of different dimensional chaotic systems. However, some of priori-unknown parameters are required to implement the update laws in Eqs. (14) and (19) in [25]. Such technical incorrectness was shown by Sun *et al.* [26]. In addition, the studies in [20]–[24] were built based on Lemma 1 in [27], which leads to the slow convergence if the initial state values are large.

Furthermore, most of the aforementioned control techniques suffered from the chattering effect due to the use of discontinuous control, $sign(\cdot)$, which can cause the significant reduction of the synchronization performance. In order to deal with this issue, researchers replaced the $sign(\cdot)$ with some smoothing approximation such as the hyperbolic, relay, or saturation function. Nevertheless, the robustness and invariant properties [28] have not been guaranteed, and the synchronization errors only enter into the neighbor centered at the origin [29].

Motivated by all the above concerns, the main object of this article is to develop a new control strategy to achieve the adaptive FT-MFPS (AFT-MFPS) of HPSs subject to external disturbance and model uncertainties. The novel contributions of this work are outlined as follows.

1) New integral fast terminal sliding mode (I-FTSM) manifolds are introduced to achieve fast convergence and high accuracy of synchronization;
2) The combination of the new I-FTSM and the adaptive second-order sliding mode algorithm (A-SOSMA) [30] relaxes the requirement of the upper bounds of unknown EDaU and results in the continuous control signals which help mitigating the chattering effect;
3) The stability of the closed-loop systems and the finite-time convergence of synchronization errors are theoretically proven; and
4) The AFT-MFPS of HPSs is obtained for the first time, which possess the following remarkable features. Firstly, while the existing approaches either do not deal with EDaU [8]–[10] or require the upper bounds of EDaU (see [11] and [12]), our approach is able to successfully synchronize the HPSs against the unknown external disturbance and uncertainties. Secondly, compared to both classic adaptive control approaches [13]–[17] and FTC ones [19]–[24] which replace $sign(\cdot)$ with some smooth approximation that only make MFPS errors either bounded or enter into the neighbor centered at the origin, all MFPS errors is ensured to reach zero in finite time by our proposed one. Lastly, the faster finite-time convergence is achieved by using the proposed I-FTSM manifolds instead of applying the existing TSM manifold [20]–[24].

The rest of this article is organized as follows. Section II describes the problem formulation and some preliminaries. Section III shows the main result including the two-step design procedure. The effectiveness of the proposed scheme is demonstrated using two illustrative simulation examples, and further applied to a practical engineering application in Section IV. Conclusions are given in Section V.

II. PROBLEM DESCRIPTION AND PRELIMINARIES

A. PROBLEM DESCRIPTION

Consider an uncertain HPS that is taken as a master system of the form

$$\begin{cases} \dot{x}_{m1} = f_{m1}(x_m, t) + d_{m1}(x_m, t), \\ \dot{x}_{m2} = f_{m2}(x_m, t) + d_{m2}(x_m, t), \\ \cdots \\ \dot{x}_{mn} = f_{mn}(x_m, t) + d_{mn}(x_m, t), \end{cases} \tag{1}$$

where $x_m = [x_{m1}, x_{m2}, \ldots, x_{mn}]^T$ is the state vector, $f_{mi}(x_m, t)$ represent known nonlinear functions, and $d_{mi}(x_m, t)$, $(i = 1, 2, \ldots, n)$ denote EDaU. The second uncertain (HPS) considered as a slave system is given by

$$\begin{cases} \dot{x}_{s1} = f_{s1}(x_s, t) + d_{s1}(x_s, t) + u_1(t), \\ \dot{x}_{s2} = f_{s2}(x_s, t) + d_{s2}(x_s, t) + u_2(t), \\ \cdots \\ \dot{x}_{sn} = f_{sn}(x_s, t) + d_{sn}(x_s, t) + u_n(t), \end{cases} \tag{2}$$

where $x_s = [x_{s1}, x_{s2}, \ldots, x_{sn}]^T$ is the state vector. Similar to the master system, the functions $f_{si}(x_s, t)$ are assumed to

be known, $d_{si}(x_s, t)$, are EDaU, and $u_i(t)$ denote the control signals.

Remark 1: The differential equation (1) is the general expression of various reported HPSs including the four-dimensional (4D) HPSs such as the Chen HPS and Lorenz HPS (see, e.g. [5], [31]–[35]) and five-dimensional (5D) HPSs [20], [36].

Based on the work of Fu [17], let us define the MFPS error (MFPSE) between (1) and (2) as

$$e_i(t) = \lambda_i \eta(t) x_{si}(t) - x_{mi}(t), \tag{3}$$

where λ_i are constants and $\eta(t)$ does not vanish at zero and is a continuously differentiable and bounded function. Therefore, the differential equation of the MFPSE dynamics raised from (1), (2), and (3) can be expressed as

$$\begin{aligned}\dot{e}_i(t) = \lambda_i \dot{\eta}(t) x_{si} - f_{mi}(x_m, t) + \lambda_i \eta(t) f_{si}(x_s, t) \\ - d_{mi}(x_m, t) + \lambda_i \eta(t) d_{si}(x_s, t) + \lambda_i \eta(t) u_i(t).\end{aligned} \tag{4}$$

In this article, the following assumption is required for the subsequent development (see [37] and [38]).

Assumption 1: It is assumed that the uncertain terms $d_{e_i}(x_m, x_s, t) = -d_{mi}(x_m, t) + \lambda_i \eta(t) d_{si}(x_s, t)$ are Lipschitz continuous functions, *i.e.*,

$$-k_{e_i} \leq \frac{d}{dt} d_{e_i}(x_m, x_s, t) \leq k_{e_i},$$

where $k_{e_i}, \forall i \in \{1, 2, \cdots, n\}$ are unknown positive constants.

Remark 2: It is not difficult to see that the considered MFPS will become the anti-synchronization (AS), the complete synchronization (CS), the projective synchronization (PS), the function PS (FPS), and the modified PS (MPS) when $\lambda_i \eta(t)$ have appropriate values, which are shown in Table 1 in detail.

TABLE 1. The synchronization types.

Synchronization type	Parameters $\lambda_i \eta(t), (i = 1, 2, \ldots, n)$
AS [39]	$\lambda_i \eta(t) = -1$
CS [40]	$\lambda_i \eta(t) = 1$
PS [41]	$\lambda_i \eta(t) = \lambda \neq 0, \forall i$
FPS [42]	$\lambda_i = 1, \forall i$ and $\eta(t) \neq 0$
MPS [43]	$\lambda_i \neq 0, \forall i$ and $\eta(t) = 1$

Let us denote the MFPSE vector by $e(t) = [e_1(t), e_2(t), \ldots, e_n(t)]^T$, and the FT-MFPS is defined as follows.

Definition 1: The FT-MFPS of the master system (1) and the slave system (2) is said to be achieved if there exists a non-negative constant T depending on the initial conditions $e(0)$ such that $e(t)$ goes to zero as $t \to T$ and remains at zero after the instance time T.

In view of Definition 1 in the connection with Definition 2 in the next subsection, our task is to suitably choose control signals $u_i(t)$ to ensure the global stability of the MFPSE dynamics (4) and to steer the MFPSE vector $e(t)$ from any initial state to the origin in finite time.

B. PRELIMINARIES

This section provides a set of definition and Lemma which will be used during the design procedure.

Definition 2 [44]: Consider the system

$$\dot{z} = \psi(t, z), \quad z_0 = z(0), \tag{5}$$

where $z \in \mathbb{R}^n$ and $\psi : \mathbb{R}_+ \times \mathbb{R}^n \to \mathbb{R}^n$, and assume the origin is the equilibrium of (5). The solutions of (5) are understood in the sense of Filippov. The origin of (5) is said to be globally finite-time stable if it is globally asymptotically stable and any solution $z(t, z_0)$ of (5) reaches the equilibria at some finite time moment, *i.e.*, $z(t, z_0) = 0, \forall t \geq T(z_0)$, where $T : \mathbb{R}^n \to \mathbb{R}_+ \cup \{0\}$ is the settling time function.

The A-SOSMA in the following Lemma is adapted from the work of Laghrouche *et al.* [30] that is inspired by the well-known super-twisting algorithm [45].

Lemma 1: Consider the system

$$\begin{cases}\dot{\zeta}_1 = -a(t) \lfloor \zeta_1 \rceil^{1/2} - k_a(t) \zeta_1 + \zeta_2, \\ \dot{\zeta}_2 = -b(t) \lfloor \zeta_1 \rceil^0 - k_b(t) \zeta_1 + \rho(t).\end{cases} \tag{6}$$

Suppose that there exists some unknown non-negative constant k_ρ such that the perturbation $|\rho(t)| \leq k_\rho$. If we define the time-varying parameters as

$$\begin{aligned} a(t) &= a_0 \sqrt{\Gamma_0(t)}, \quad b(t) = b_0 \Gamma_0(t), \\ k_a(t) &= k_{a_0} \Gamma_0(t), \quad k_b(t) = k_{b_0} \Gamma_0^2(t), \end{aligned} \tag{7}$$

with the update law

$$\dot{\Gamma}_0(t) = \begin{cases} k_{\Gamma_0}, & \text{if } |\zeta_1| \neq 0 \\ 0, & \text{else,} \end{cases} \tag{8}$$

where $a_0, b_0, k_{a_0}, k_{b_0}$, and k_{Γ_0} are designed positive parameters satisfying the following condition

$$4 b_0 k_{b_0} > 8 b_0 k_{a_0}^2 + 9 a_0^2 k_{a_0}^2. \tag{9}$$

The state trajectories of (6) tend to zero in finite time.

Throughout this article, we use the notation $\lfloor x \rceil^\gamma = |x|^\gamma \text{sign}(x)$, where $\gamma \geq 0$ (see [46]). For a brief expression, let d_{e_i}, e_i and u_i denote $d_{e_i}(x_m, x_s, t), e_i(t)$ and $u_i(t)$, respectively, unless explicitly expressed.

III. MAIN RESULTS

The whole structure of the AFT-MFPS control strategy is shown in Fig. 1. The detailed description of two-step design procedure of the proposed synchronizing control strategy is given in this section. First, we introduce appropriate I-FTSM manifolds that exhibit the desirable dynamic behavior when the sliding motion takes place. Second, the control action is established to exhibit the sliding motion in finite time and maintain such a motion.

A. DESIGN OF I-FTSM MANIFOLDS

For the MFPSE system (4), the novel I-FTSM manifolds are proposed as

$$\sigma_i = e_i - e_i(0) + \int_0^t \left(c_{1i} \mathbf{e}^{\chi_i |e_i|} e_i + c_{2i} \lfloor e_i \rceil^{\gamma_i} \right) d\tau, \tag{10}$$

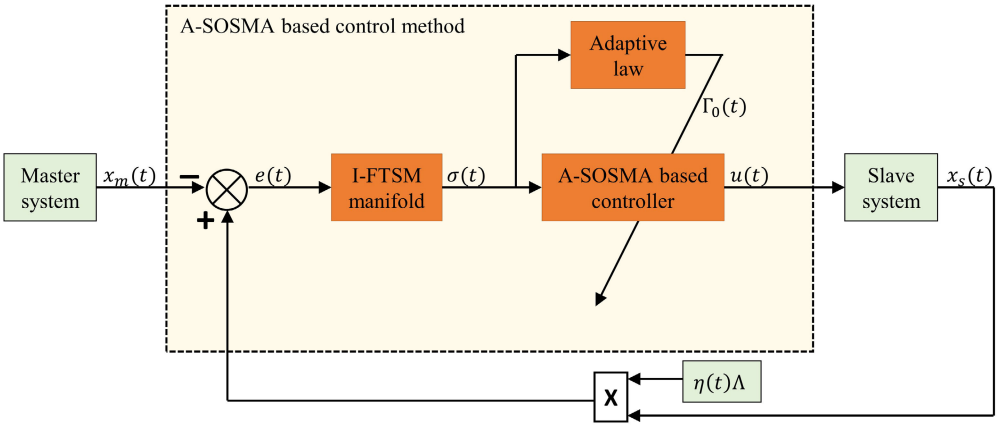

FIGURE 1. Block diagram of the proposed AFT-MFPS strategy ($\Lambda = diag(\lambda_1, \lambda_2, \ldots, \lambda_n)$).

where c_{1i}, c_{2i}, and χ_i are positive constants, $0 < \gamma_i < 1$, and $\mathbf{e}$ is Euler's number.

Remark 3: The term $c_{1i}\mathbf{e}^{\chi_i|e_i|}e_i$ helps increasing the convergence rate in the sense of self-tuning gain when the MFPSE $|e_i|$ is much bigger than 1; $\lfloor e_i \rceil^{\gamma_i}$ holds the crucial role in the period of the finite-time convergence when e_i is closed to zero.

From the sliding mode control theory [47], the presence of appropriate sliding motion yields

$$\sigma_i = 0 \text{ and } \dot{\sigma}_i = 0, \tag{11}$$

and it follows that

$$\dot{e}_i = -c_{1i}\mathbf{e}^{\chi_i|e_i|}e_i - c_{2i}\lfloor e_i \rceil^{\gamma_i}, \tag{12}$$

which is known as the sliding mode dynamics.

Theorem 1: The zero solutions of (12) are globally finite-time stable and the state trajectories of the system (12) reach zero at most after T_{e_i} given by

$$T_{e_i} = T_{\sigma_i} + \frac{1}{c_{1i}(1-\gamma_i)} \ln\left(\frac{c_{1i}}{c_{2i}}|e_{i0}|^{1-\gamma_i} + 1\right), \tag{13}$$

where T_{σ_i} is the instance time when the sliding mode motions take place.

Proof: Let the function $V_1 = \frac{1}{2}e_i^2$ be a candidate Lyapunov function for (12). Taking the total derivative along the system trajectories yields

$$\begin{aligned}\dot{V}_1 &= e_i\dot{e}_i \\ &= e_i\left(-c_{1i}\mathbf{e}^{\chi_i|e_i|}e_i - c_{2i}\lfloor e_i \rceil^{\gamma_i}\right) \\ &= -c_{1i}\mathbf{e}^{\chi_i|e_i|}e_i^2 - c_{2i}|e_i|^{\gamma_i+1} \\ &\le -2c_{1i}V_1 - 2^{\frac{\gamma_i+1}{2}}c_{2i}V_1^{\frac{\gamma_i+1}{2}}.\end{aligned} \tag{14}$$

Hence, $\dot{V}_1$ is a negative definite function, which implies that $e_i = 0$ is globally asymptotically stable.

In view of Definition 2, the last step for completing the proof of Theorem 1 is that all trajectories of (12) should be ensured to reach zero at some amount of finite time. Consider the nonlinear system described by the differential equation

$$\dot{\xi} = -\lambda_1\xi - \lambda_2\xi^{\nu}, \quad \xi_0 = \xi(t_0) \ge 0, \tag{15}$$

where t_0 is the initial time, λ_1 and λ_2 are positive values, and $0 < \nu < 1$. Since V_1 is positive definite, it is sufficient to solve for (15) based upon the assumption $\xi \in \mathbb{R}_+ \cup \{0\}$.

We can write the differential equation (15) as

$$\frac{d\xi}{\lambda_1\xi + \lambda_2\xi^{\nu}} = -dt, \tag{16}$$

then

$$\frac{1}{\lambda_1(1-\nu)}\frac{d\left(\lambda_1\xi^{1-\nu} + \lambda_2\right)}{\lambda_1\xi^{1-\nu} + \lambda_2} = -dt. \tag{17}$$

Integrating both sides of the above equation yields the solution of (15) in the form of

$$\begin{aligned}&\xi(t, \xi_0) \\ &= \begin{cases}\left[\dfrac{\left(\lambda_1\xi_0^{1-\nu} + \lambda_2\right)\mathbf{e}^{-\lambda_1(1-\nu)(t-t_0)} - \lambda_2}{\lambda_1}\right]^{\frac{1}{1-\nu}}, & t \le T_{\xi}, \\ 0, & t > T_{\xi},\end{cases}\end{aligned} \tag{18}$$

where $T_{\xi} = t_0 + \frac{1}{\lambda_1(1-\nu)}\ln\left(\frac{\lambda_1\xi^{1-\nu}+\lambda_2}{\lambda_2}\right)$. This settling time is similar to the result in Remark 2 in [29].

Now, inspired by the proof of Theorem 2 in [45], by invoking the comparison principle [48], it can be shown that $V_1 \le \xi(t, \xi_0)$ when $V_1(e_{i0}) \le \xi_0$, where $e_{i0} = e_i(t = t_0)$. It follows, from (14) and (18), that $e_i(t)$ go to zero at most after a finite time satisfying

$$\begin{aligned}T_{e_i} &= T_{\sigma_i} + \frac{1}{c_{1i}(1-\gamma_i)}\ln\left(2^{\frac{1-\gamma_i}{2}}\frac{c_{1i}}{c_{2i}}V_1(e_{i0})^{\frac{1-\gamma_i}{2}} + 1\right) \\ &= T_{\sigma_i} + \frac{1}{c_{1i}(1-\gamma_i)}\ln\left(\frac{c_{1i}}{c_{2i}}|e_{i0}|^{1-\gamma_i} + 1\right),\end{aligned}$$

where $t_0 = T_{\sigma_i}$. ■

Remark 4: Referring to the studies in [29], [49], [50] and [20]–[25], some integral TSM/FTSM could be summarized as in Table 2. The convergence rate of the proposed I-FTSM surfaces (10) are faster than any of those in Table 1 because of Remark 3 and the effect of the exponential term $\mathbf{e}^{\chi_i|e_i|}$ that could be considered as a self-tuning gain. If the initial states are far away from zero, the exponential term has a big value which facilitates increasing the convergence speed.

TABLE 2. The TSM/FTSM manifolds.

TSM/FTSM Manifold	Description [a]
Integral TSM [49]	$\sigma_i = e_i + \int_0^t \mu e_i^{p_2/p_1} d\tau$
Integral FTSM [50]	$\sigma_i = e_i + \int_0^t \left(\mu_1 e_i + \mu_2 e_i^{p_2/p_1}\right) d\tau$
Integral TSM [29]	$\sigma_i = e_i + \int_0^t \mu \lfloor e_i \rceil^{\gamma} d\tau$
Integral FTSM [29]	$\sigma_i = e_i + \int_0^t (\mu_1 e_i + \mu_2 \lfloor e_i \rceil^{\gamma}) d\tau$

[a] The design parameters: $\mu > 0, \mu_1 > 0, \mu_2 > 0, p_1$ and p_2 are odd integers, $p_1 > p_2 > 0$, and $0 < \gamma < 1$.

B. DESIGN OF CONTROL LAWS

In this subsection, we employ the proposed I-FTSM manifolds for the MFPSE (4) and design control laws that make the I-FTSM variables σ_i reach zero at some finite amount of time. The following Theorem describes the structure of the proposed controller in detail.

Theorem 2: Consider system (4) with the lumped uncertainty satisfying Assumption 1. If the proposed control input signals are defined as (19) whose design parameters are adjusted according to (7), (8) and satisfy (9), the I-FTSM variables converge to zero in certain finite time T_{σ_i}.

$$\begin{aligned} u_i(t) = -f_{si}(x_s, t) - \frac{1}{\lambda_i \eta(t)} \Big\{ & \lambda_i \dot{\eta}(t) x_{si} - f_{mi}(x_m, t) \\ & + c_{1i} \mathbf{e}^{\chi_i |e_i|} e_i + c_{2i} \lfloor e_i \rceil^{\gamma_i} + a(t) \lfloor \sigma_i \rceil^{1/2} + k_a(t) \sigma_i \\ & - \int_0^t \left[b(t) \lfloor \sigma_i \rceil^0 + k_b(t) \sigma_i \right] d\tau \Big\}. \end{aligned} \tag{19}$$

Proof: From (4) and (12), it can be shown that

$$\begin{aligned} \dot{\sigma}_i &= \dot{e}_i + c_{1i} \mathbf{e}^{\chi_i |e_i|} e_i + c_{2i} \lfloor e_i \rceil^{\gamma_i} \\ &= \lambda_i \dot{\eta}(t) x_{si} - f_{mi}(x_m, t) \\ &\quad + \lambda_i \eta(t) f_{si}(x_s, t) + d_{e_i} \\ &\quad + \lambda_i \eta(t) u_i(t) + c_{1i} \mathbf{e}^{\chi_i |e_i|} e_i + c_{2i} \lfloor e_i \rceil^{\gamma_i}. \end{aligned} \tag{20}$$

Then, using the control laws (19), the above equation leads to

$$\begin{aligned} \dot{\sigma}_i = & -a(t) \lfloor \sigma_i \rceil^{1/2} - k_a(t) \sigma_i \\ & - \int_0^t \left[b(t) \lfloor \sigma_i \rceil^0 + k_b(t) \sigma_i \right] d\tau + d_{e_i}, \end{aligned} \tag{21}$$

and it follows that

$$\begin{cases} \dot{\sigma}_i = -a(t) \lfloor \sigma_i \rceil^{1/2} - k_a(t) \sigma_i + \vartheta, \\ \dot{\vartheta} = -b(t) \lfloor \sigma_i \rceil^0 - k_b(t) \sigma_i + \frac{d}{dt} d_{e_i}, \end{cases} \tag{22}$$

where

$$\vartheta = -\int_0^t \left[b(t) \lfloor \sigma_i \rceil^0 + k_b(t) \sigma_i \right] d\tau + d_{e_i}.$$

Hence, by invoking Lemma 1 in the connection with Assumption 1, we conclude that all state trajectories of (22) goes to zero in finite time. This implies that the finite-time convergence of the I-FTSM variables is achieved, (*i.e.*, $\sigma_i = 0$) at most after T_{σ_i}. ■

Remark 5: In view of Theorems 1 and 2, it is clear that the proposed strategy ensures that the AFT-MFPS between HPSs (1) and (2) is obtained at most after T satisfying $T \leq \max_{i=1,2,\ldots,n} \{T_{e_i}\}$.

Remark 6: The chattering effect is substantially alleviated because of the continuity of the suggested control input signals (19).

Remark 7: If there are no effects of EDaU on the synchronized HPSs (*i.e.*, $d_{e_i} = 0$), the second-order sliding mode in (22) will be maintained from the beginning (*i.e*, $\sigma_i = \dot{\sigma}_i \equiv 0, \forall t \geq t_0$), which implies that the differential equation (12) exhibits the behavior of the closed-loop system.

IV. SIMULATION RESULTS

To further validate the benefit of the proposed algorithm, two illustrative examples are numerically demonstrated and analyzed in detail. The first example considers the FT-MFPS of uncertain HPSs and the second one studies the finite-time CS (FTCS) of 5D HPSs. In addition, a secure communication system using 5D HPSs is built to illustrate the application of the method. The Runge-Kutta integration routine with a sample time of $10^{-3}(s)$ is used in all the simulations.

A. EXAMPLE 1

We consider the first example in which the simulation results of the suggested controller employed for the FT-MFPS of two systems: the uncertain hyperchaotic Lü system [31] as the master system and the uncertain hyperchaotic Lorenz system [32] as the slave system. Besides, a comparison with a new control technique recently developed in [17] is performed to illustrate the standout control properties of the proposed control strategy.

The master system is

$$\dot{x}_m = f_m(x_m) + d_m(x_m), \tag{23}$$

where

$$x_m = [x_{m1}, x_{m2}, x_{m3}, x_{m4}]^T,$$

$$f_m(x_m) = \begin{bmatrix} f_{m1}(x_m) \\ f_{m2}(x_m) \\ f_{m3}(x_m) \\ f_{m4}(x_m) \end{bmatrix} = \begin{bmatrix} x_{m4} \\ -x_{m1} x_{m3} \\ x_{m1} x_{m2} \\ x_{m1} x_{m3} \end{bmatrix},$$

$$d_m(x_m) = \begin{bmatrix} d_{m1}(x_m) \\ d_{m2}(x_m) \\ d_{m3}(x_m) \\ d_{m4}(x_m) \end{bmatrix} = \begin{bmatrix} 36(x_{m2} - x_{m1}) \\ 20 x_{m2} \\ -3 x_{m3} \\ x_{m4} \end{bmatrix}.$$

The slave system is given by

$$\dot{x}_s = f_s(x_s) + d_s(x_s, t) + u(t), \tag{24}$$

where

$$
\begin{aligned}
x_s &= [x_{s1}, x_{s2}, x_{s3}, x_{s4}]^T, \\
f_s(x_s) &= \begin{bmatrix} f_{s1}(x_s) \\ f_{s2}(x_s) \\ f_{s3}(x_s) \\ f_{s4}(x_s) \end{bmatrix} = \begin{bmatrix} x_{s4} \\ -x_{s2} - x_{s1}x_{s3} \\ x_{s1}x_{s2} \\ -x_{s2}x_{s3} \end{bmatrix}, \\
d_s(x_s, t) &= \begin{bmatrix} d_{s1}(x_s, t) \\ d_{s2}(x_s, t) \\ d_{s3}(x_s, t) \\ d_{s4}(x_s, t) \end{bmatrix} \\
&= \begin{bmatrix} 10(x_{s2} - x_{s1}) - 0.5\sin(0.25\pi t) \\ 28x_{s1} + 0.2\cos(5\pi t) \\ -8/3x_{s3} + 1.8\sin(6\pi t) \\ -0.5x_{s4} + 2\cos(2\pi t) \end{bmatrix}, \\
u(t) &= [u_1, u_2, u_3, u_4]^T.
\end{aligned}
$$

Let the initial states be $x_m(0) = [1, -1, 1, -1]^T$ and $x_s(0) = [-1, 1, -2, 1]^T$. The scaling parameters and scaling function in (3) are set as $(\lambda_1, \lambda_2, \lambda_3, \lambda_4) = (5, -1, -3, 4)$ and $\eta(t) = 5 + \sin(0.2\pi t)$, respectively. From (23) and (24), the lumped uncertain terms are described by $d_{e_i} = -d_{mi}(x_m) + \lambda_i \eta(t) d_{si}(x_s, t)$ that are shown in Fig. 2, which implies that Assumption 1 is satisfied.

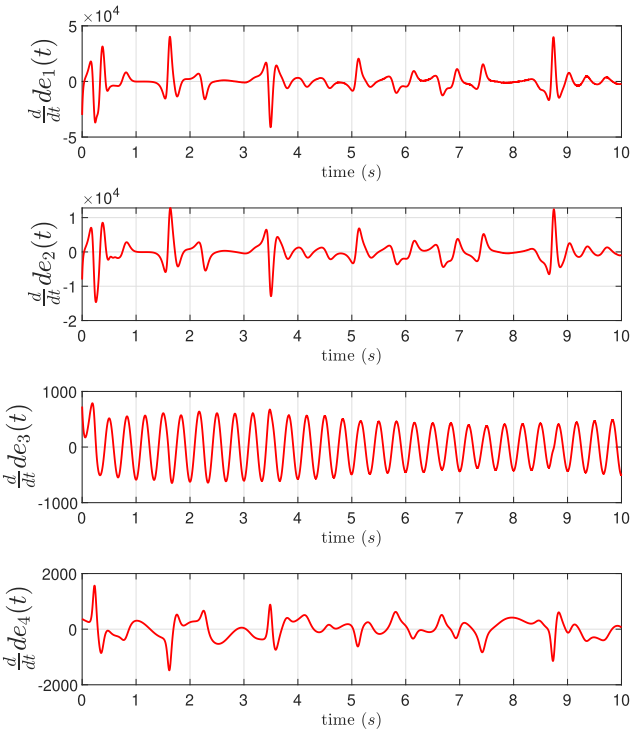

FIGURE 2. The time evolution of the first derivative of the lumped uncertain term.

We apply the proposed control algorithm (7), (8), (9), (10), and (19) by choosing $a_0 = 2, b_0 = 14, k_{a_0} = 2.5, k_{b_0} = 30, k_{\Gamma_0} = 20, c_{1i} = 0.002, c_{21} = c_{22} = 30, c_{23} = c_{24} = 10, \chi_i = 0.01, \gamma_i = 3/5, (i = 1, 2, 3, 4)$ and the initial condition of $\Gamma_0(0) = 2$.

The proposed controller is compared with the recently reported method in [17], designed as

$$
\begin{aligned}
u_1 &= \frac{1}{\lambda_1 \eta(t)} \left[\hat{a}_1(x_{m2} - x_{m1}) + x_{m4} - \lambda_1 \dot{\eta}(t) x_{s1} - k e_1\right] \\
&\quad -\hat{a}_2(x_{s2} - x_{s1}) - x_{s4} - \rho_1 \text{sign}\left(\lambda_1 \eta(t) e_1\right), \\
u_2 &= \frac{1}{\lambda_2 \eta(t)} \left[-x_{m1}x_{m3} + \hat{c}_1 x_{m2} - \lambda_2 \dot{\eta}(t) x_{s2} - k e_2\right] \\
&\quad -\hat{c}_2 x_{s1} + x_{s2} + x_{s1}x_{s3} - \rho_2 \text{sign}\left(\lambda_2 \eta(t) e_2\right), \\
u_3 &= \frac{1}{\lambda_3 \eta(t)} \left[x_{m1}x_{m2} - \hat{b}_1 x_{m3} - \lambda_3 \dot{\eta}(t) x_{s3} - k e_3\right] \\
&\quad -x_{s1}x_{s2} + \hat{b}_2 x_{s3} - \rho_3 \text{sign}\left(\lambda_3 \eta(t) e_3\right), \\
u_4 &= \frac{1}{\lambda_3 \eta(t)} \left[x_{m1}x_{m3} + \hat{r}_1 x_{m4} - \lambda_4 \dot{\eta}(t) x_{s4} - k e_4\right] \\
&\quad +x_{s2}x_{s3} - \hat{r}_2 x_{s4} - \rho_4 \text{sign}\left(\lambda_4 \eta(t) e_4\right),
\end{aligned} \tag{25}
$$

with the update gains as

$$
\begin{aligned}
\dot{\hat{a}}_1 &= -e_1(x_{m2} - x_{m1}), \\
\dot{\hat{a}}_2 &= \lambda_1 \eta(t) e_1 (x_{s2} - x_{s1}), \\
\dot{\hat{b}}_1 &= e_3 x_{m3}, \quad \dot{\hat{b}}_2 = -\lambda_3 \eta(t) e_3 x_{s3}, \\
\dot{\hat{c}}_1 &= -e_2 x_{m2}, \quad \dot{\hat{c}}_2 = \lambda_2 \eta(t) e_2 x_{s1}, \\
\dot{\hat{r}}_1 &= -e_4 x_{m4}, \quad \dot{\hat{r}}_2 = \lambda_4 \eta(t) e_4 x_{s4}.
\end{aligned} \tag{26}
$$

The initial values of the unknown parameters are $\hat{a}_1(0) = \hat{b}_1(0) = \hat{c}_1(0) = \hat{r}_1(0) = \hat{a}_2(0) = \hat{b}_2(0) = \hat{c}_2(0) = \hat{r}_2(0) = 1$ and $k(0) = 2$. The controller in [17] is designed assuming that the boundaries of the external disturbances are known as a priori, that is, $\rho_1 = 0.5, \rho_2 = 0.2, \rho_3 = 1.8$, and $\rho_4 = 2$. For fair comparison, these design parameters as well as the simulation environment are the same as those used in [17].

The simulation results of the proposed strategy are presented in Figs. 3-5. The time evolution of the FT-MFPS errors is displayed in Fig.3, in which all of the synchronization errors with the proposed control method converge to zero quickly in finite time. It means that the FT-MFPS between the Lü system system and Lorenz system is achieved. Moreover, the proposed control strategy can accomplish superior control performance with much smaller synchronization errors compared with the control technique in [17]. The results of control input in Fig. 4 show that the chattering phenomenon is eliminated by applying the proposed technique. Further, in comparison with the strategy in [17], the proposed control technique can provide smoother control inputs. Note that the control laws (25) utilized sign(·) discontinuous functions that will cause chattering phenomenon whenever the

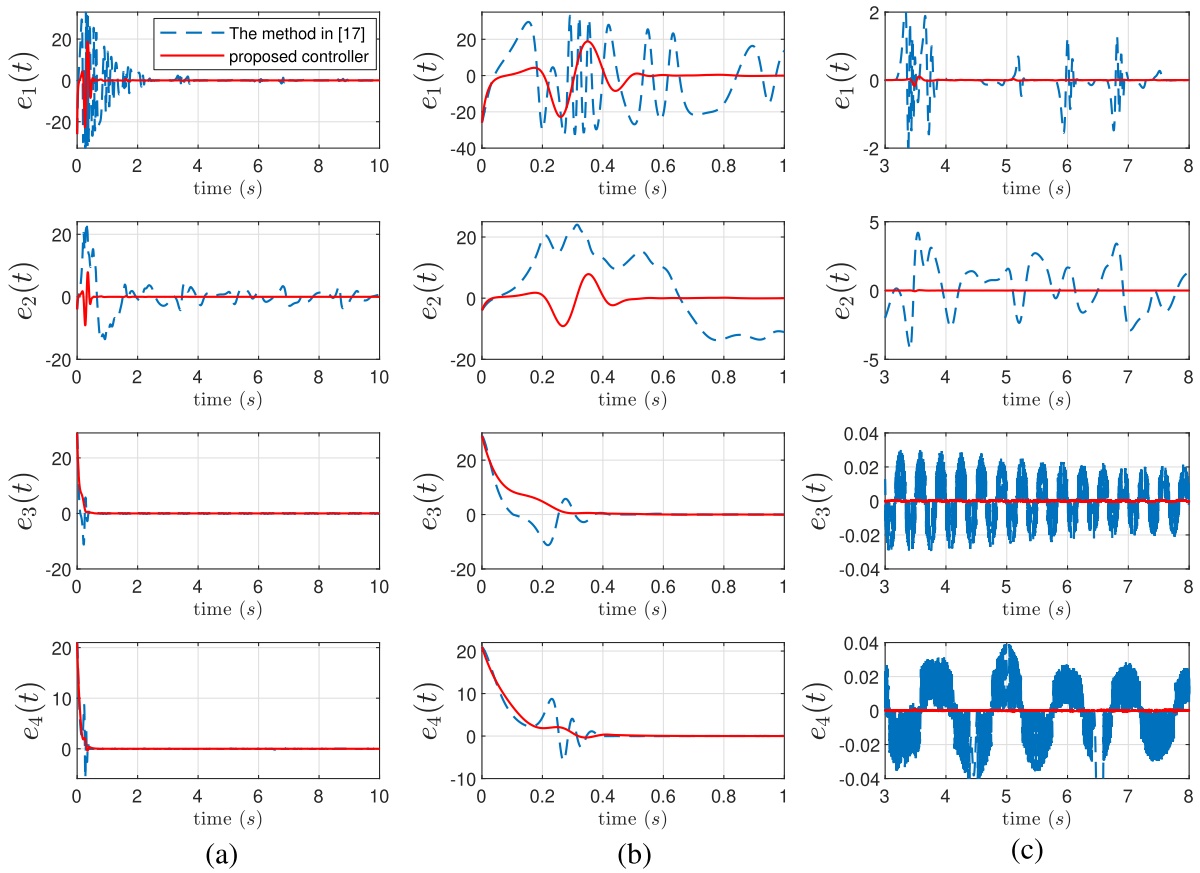

FIGURE 3. The FT-MFPS errors: Column (a) depicts $e(t)$ in normal scale, Column (b) depicts $e(t)$ in a time interval [0, 1] enlarged, and Column (c) depicts $e(t)$ in a time interval [3, 8] enlarged.

external disturbances are big. The fine-time convergence of the non-singular terminal sliding manifolds is illustrated in Fig. 5.

B. EXAMPLE 2

The second example investigates the FTCS of 5D Lorenz-like systems [36] without uncertainties and external disturbances to illustrate the statement in Remark 7. In comparison with the recently introduced passivity technique-based method [20], we will show that the proposed strategy possesses the superior performance.

The dynamics of the master system has the form

$$\dot{x}_m = f_m(x_m), \tag{27}$$

where

$$x_m = [x_{m1}, x_{m2}, \ldots, x_{m5}]^T,$$
$$f_m(x_m) = \begin{bmatrix} f_{m1}(x_m) \\ f_{m2}(x_m) \\ f_{m3}(x_m) \\ f_{m4}(x_m) \\ f_{m5}(x_m) \end{bmatrix} = \begin{bmatrix} 10(x_{m2} - x_{m1} + x_{m4} \\ 28x_{m1} - x_{m1}x_{m3} + x_{m5} \\ -\frac{8}{3}x_{m3} + x_{m1}x_{m2} \\ 2x_{m4} - x_{m1}x_{m3} \\ 0.09x_{m1} - 8x_{m2} \end{bmatrix},$$

and the slave system is represented in the form

$$\dot{x}_s = f_s(x_s) + u(t), \tag{28}$$

where

$$x_s = [x_{s1}, x_{s2}, \ldots, x_{s5}]^T,$$
$$u(t) = [u_1, u_2, \ldots, u_5]^T,$$
$$f_s(x_s) = \begin{bmatrix} f_{s1}(x_s) \\ f_{s2}(x_s) \\ f_{s3}(x_s) \\ f_{s4}(x_s) \\ f_{s5}(x_s) \end{bmatrix} = \begin{bmatrix} 10(x_{s2} - x_{s1} + x_{s4} \\ 28x_{s1} - x_{s1}x_{s3} + x_{s5} \\ -\frac{8}{3}x_{s3} + x_{s1}x_{s2} \\ 2x_{s4} - x_{s1}x_{s3} \\ 0.09x_{s1} - 8x_{s2} \end{bmatrix}.$$

As mentioned in Remark 2, the CS error is given by $e(t) = x_s(t) - x_m(t)$ corresponding to (3) with $\lambda_i \eta(t) = 1$. Thus, the CS error dynamics in this example is obtained as follows (also see [20])

$$\begin{cases} \dot{e}_1 = 10(e_2 - e_1) + e_4 + u_1, \\ \dot{e}_2 = 28e_1 - e_1e_3 - e_1x_{m3} - e_3x_{m1} + e_5 + u_2, \\ \dot{e}_3 = -\frac{8}{3}e_3 + e_1e_2 + e_2x_{m1} + e_1x_{m2} + u_3, \\ \dot{e}_4 = 2e_4 - e_1e_3 - e_1x_{m3} - e_3x_{m1} + u_4, \\ \dot{e}_5 = 0.09e_1 - 8e_2 + u_5. \end{cases} \tag{29}$$

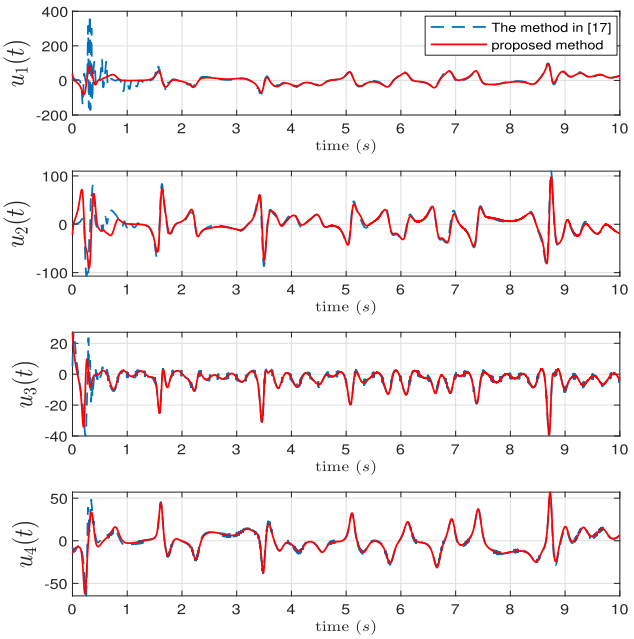

FIGURE 4. The control input evolution with respect to time for the FT-MFPS.

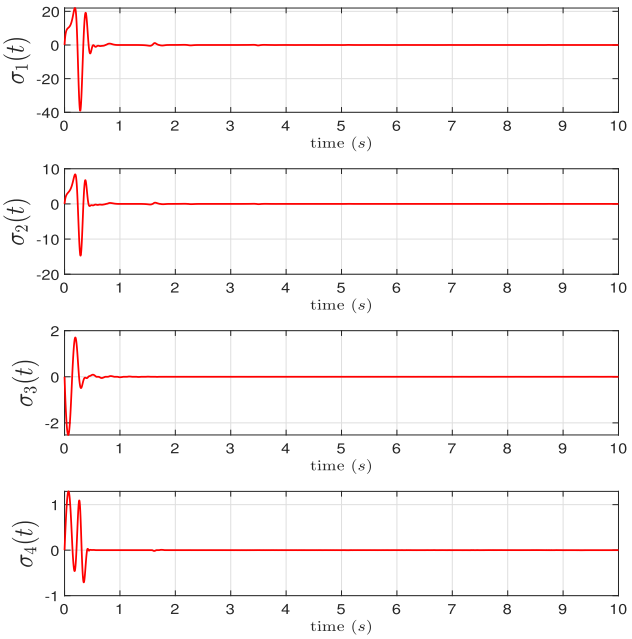

FIGURE 5. The I-FTSM manifolds for the FT-MFPS.

The initial states are set $x_m(0) = [15, -18, -16, 10, 13]^T$ and $x_s(0) = [2, 1, 0, 2, 2]^T$. The design parameters in (7), (8), (9), (10), and (19) are set as $a_0 = 2$, $b_0 = 14$, $k_{a_0} = 2.5$, $k_{b_0} = 30$, $k_{\Gamma_0} = 20$, $c_{1i} = 10$, $c_{2i} = 60$, $\chi_i = 0.01$, $\gamma_i = 3/5$, $(i = 1, 2, 3, 4, 5)$ and the initial condition of $\Gamma_0(0) = 2$. Sangpet and Kuntanapreeda [20] introduced a passivity approach-based controller for the CS, designed as

$$\begin{aligned}
u_1 &= -\alpha_1 \lfloor e_1 \rceil^{\eta_0}, \\
u_2 &= -28e_1 - e_1 x_{m3} + 7e_5 - \frac{3\bar{x}_{m2}}{16} e_1 - \beta_1 \lfloor e_1 \rceil^{\eta_0}, \\
u_3 &= -\alpha_2 \lfloor e_3 \rceil^{\eta_0}, \\
u_4 &= -2e_4 + e_1 e_3 + e_1 x_{m3} + e_3 x_{m1} \\
&\quad - \frac{3\bar{x}_{m2}}{160} e_1 - \beta_2 \lfloor e_4 \rceil^{\eta_0}, \\
u_5 &= -0.09e_1 - \beta_3 \lfloor e_5 \rceil^{\eta_0},
\end{aligned} \tag{30}$$

where $\alpha_1 = 22.9, \alpha_2 = \beta_1 = \beta_2 = \beta_3 = 40.3, \bar{x}_{m2} = 30$, and $\eta_0 = 3/5$. Note that these design parameters are taken directly from the simulation section in [20] to provide a fair comparison.

Figures 6-8 show the simulation results. From the responses of the CS errors in Fig. 6, we can see that the proposed control algorithm is better than the passivity approach in [20] in both the transient and steady-state performance. By defining the I-FTSM manifolds as (10) and without the effects of uncertainties and external disturbances, the I-FTSM manifold variables are equal to zero from the start as mentioned in Remark 7 that is confirmed by Fig. 8. Therefore, the exponential decay of the CS errors in Fig. 6 is not surprising when observing the description of the closed-loop system given by (12). The faster convergence of the proposed control confirms what is stated in Remark 4. In addition, the finite-time stability in [20] does not hold if uncertainties and/or external disturbances affect the synchronized systems, whereas the proposed approach does as shown in the previous example.

C. APPLICATION TO SECURE COMMUNICATION SYSTEM

By using the 5D Lorenz-like system in Subsection IV-B, this subsection describes a secure communication system to demonstrate the application of the suggested AFT-MFPS control algorithm. This engineering application is inspired by the work of Modiri and Mobayen [51]. The information-bearing signal $h(t)$ is described by the sinc function as follows (see [51])

$$h(t) = \frac{150 \sin(4\pi(t - \pi))}{4\pi(t - \pi)}. \tag{31}$$

At the transmitter side, the signal $h(t)$ is encoded as (see [52])

$$h_{en}(t) = x_{m1}^2 + \left(1 + x_{m1}^2\right) h(t), \tag{32}$$

where $h_{en}(t)$ denotes the encrypted signal and x_{m1} is the state variable of (27). Using the similar method as in [51], the encrypted signal $h_{en}(t)$ and the type of the hyperchaotic system are transmitted to the receiver. At the receiver side, the information signal is reconstructed by (see [52])

$$\tilde{h}(t) = -\frac{x_{s1}^2}{1 + x_{s1}^2} + \frac{h_{en}(t)}{1 + x_{s1}^2}, \tag{33}$$

where $\tilde{h}(t)$ represents the recovered signal and x_{s1} is the state variable of (28). It is easy to show that the recovered signal $\tilde{h}(t)$ is identical to the original information signal $h(t)$ from the time that the FTCS in Subsection IV-B is achieved, *i.e.*, $x_{s1} \equiv x_{m1}$.

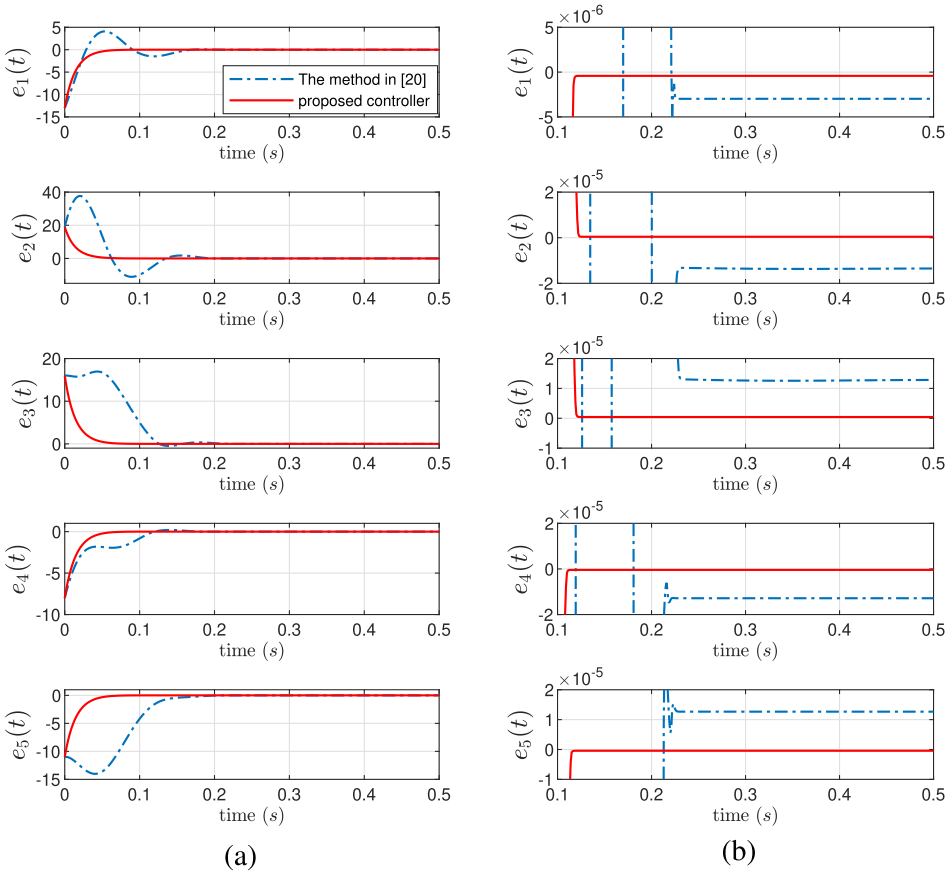

FIGURE 6. The CS errors: Column (a) depicts $e(t)$ in normal scale and Column (b) depicts $e(t)$ in a time interval [0.1, 0.5] enlarged.

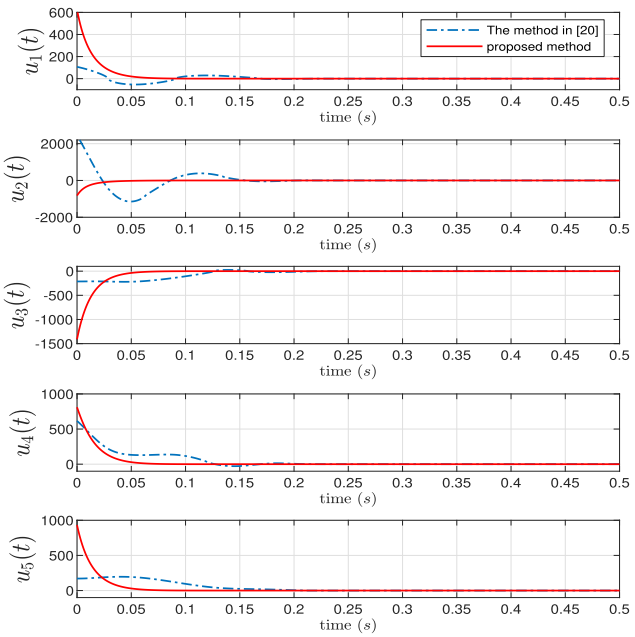

FIGURE 7. The control input evolution with respect to time for the FTCS.

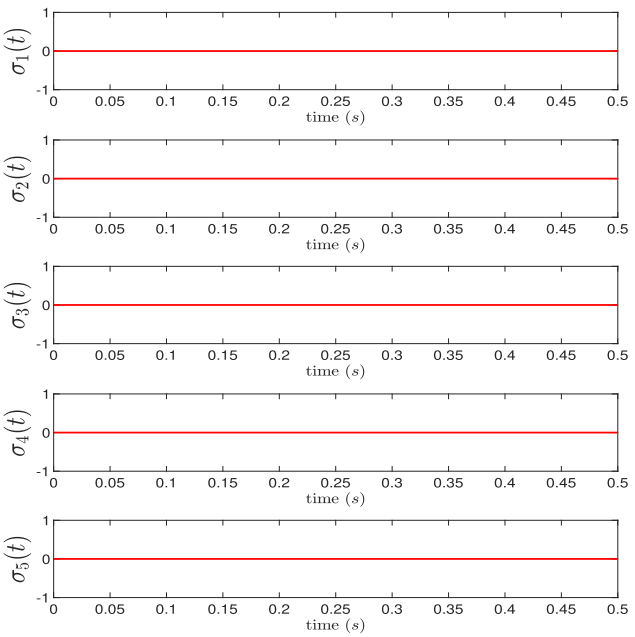

FIGURE 8. The I-FTSM manifolds for the FTCS.

Figure 9 shows numerical simulations of the secure communication system using the 5D Lorenz-like system. It is clear that, after the transient behavior, the decryption error quickly reaches zero, which implies that the the information-bearing signal are recovered almost perfectly at the receiver side.

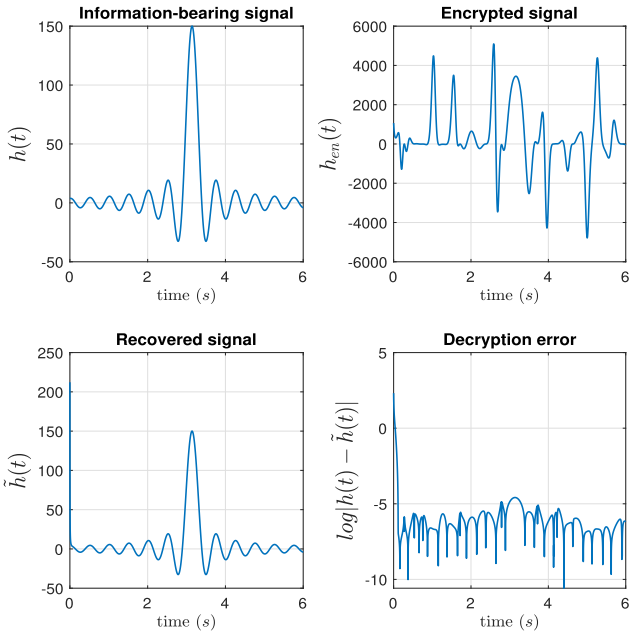

FIGURE 9. Secure communication system using 5D Lorenz-like system.

V. CONCLUSION

In this study, the challenge of the adaptive finite-time synchronization problem between different uncertain HPSs has been investigated, for which a novel AFT-MFPS control algorithm has been proposed. The superior performance of the proposed control strategy has been theoretically verified and further numerically validated by comparing with the recent studies in [17] and [20], and a secure communication system has been built to demonstrate its practical application. It is worth noting that the proposed control strategy could be easily extended to other types of synchronization or chaos control problem. Future work will include investigating the usage of the suggested method in real experiments using relevant application domains [1]–[6]. In addition, the development of this method to the case of chaotic systems with a higher relative degree is another possible future research direction.

REFERENCES

[1] G. Chen and X. Dong, *From Chaos to Order: Methodologies, Perspectives and Applications*, vol. 24. Singapore: World Scientific, 1998.

[2] W. Yan and Q. Ding, "A new matrix projective synchronization and its application in secure communication," *IEEE Access*, vol. 7, pp. 112977–112984, 2019.

[3] S. Hashemi, M. A. Pourmina, S. Mobayen, and M. R. Alagheband, "Design of a secure communication system between base transmitter station and mobile equipment based on finite-time chaos synchronisation," *Int. J. Syst. Sci.*, vol. 51, no. 11, pp. 1969–1986, Aug. 2020, Accessed: Jun. 19, 2020, doi: 10.1080/00207721.2020.1781290.

[4] S. Liu, N. Jiang, A. Zhao, Y. Zhang, and K. Qiu, "Secure optical communication based on cluster chaos synchronization in semiconductor lasers network," *IEEE Access*, vol. 8, pp. 11872–11879, 2020.

[5] M. Zhou and C. Wang, "A novel image encryption scheme based on conservative hyperchaotic system and closed-loop diffusion between blocks," *Signal Process.*, vol. 171, Jun. 2020, Art. no. 107484.

[6] H.-T. Yau, C.-C. Wang, J.-Y. Chang, and X.-Y. Su, "A study on the application of synchronized chaotic systems of different fractional orders for cutting tool wear diagnosis and identification," *IEEE Access*, vol. 7, pp. 15903–15911, 2019.

[7] X.-T. Tran and H.-J. Kang, "A novel observer-based finite-time control method for modified function projective synchronization of uncertain chaotic (hyperchaotic) systems," *Nonlinear Dyn.*, vol. 80, nos. 1–2, pp. 905–916, Apr. 2015.

[8] K. S. Sudheer and M. Sabir, "Modified function projective synchronization of hyperchaotic systems through open-plus-closed-loop coupling," *Phys. Lett. A*, vol. 374, nos. 19–20, pp. 2017–2023, Apr. 2010.

[9] A. Buscarino, L. Fortuna, and L. Patanè, "Master-slave synchronization of hyperchaotic systems through a linear dynamic coupling," *Phys. Rev. E, Stat. Phys. Plasmas Fluids Relat. Interdiscip. Top.*, vol. 100, no. 3, p. 32215, Sep. 2019.

[10] X. Chen, T. Weng, C. Gu, and H. Yang, "Synchronizing hyperchaotic subsystems with a single variable: A reservoir computing approach," *Phys. A, Stat. Mech. Appl.*, vol. 534, Nov. 2019, Art. no. 122273.

[11] S. Mobayen and F. Tchier, "Composite nonlinear feedback control technique for master/slave synchronization of nonlinear systems," *Nonlinear Dyn.*, vol. 87, no. 3, pp. 1731–1747, Feb. 2017.

[12] S. Mobayen and F. Tchier, "Synchronization of a class of uncertain chaotic systems with Lipschitz nonlinearities using state-feedback control design: A matrix inequality approach," *Asian J. Control*, vol. 20, no. 1, pp. 71–85, Jan. 2018.

[13] K. S. Sudheer and M. Sabir, "Switched modified function projective synchronization of hyperchaotic Qi system with uncertain parameters," *Commun. Nonlinear Sci. Numer. Simul.*, vol. 15, no. 12, pp. 4058–4064, Dec. 2010.

[14] S. Zheng, G. Dong, and Q. Bi, "Adaptive modified function projective synchronization of hyperchaotic systems with unknown parameters," *Commun. Nonlinear Sci. Numer. Simul.*, vol. 15, no. 11, pp. 3547–3556, Nov. 2010.

[15] Y.-H. Xu, W.-N. Zhou, and J.-A. Fang, "Modified scaling function projective synchronization of chaotic systems," *Chin. Phys. B*, vol. 20, no. 9, p. 90509, 2011.

[16] Z. Sun, G. Si, F. Min, and Y. Zhang, "Adaptive modified function projective synchronization and parameter identification of uncertain hyperchaotic (chaotic) systems with identical or non-identical structures," *Nonlinear Dyn.*, vol. 68, no. 4, pp. 471–486, Jun. 2012.

[17] G. Fu, "Robust adaptive modified function projective synchronization of different hyperchaotic systems subject to external disturbance," *Commun. Nonlinear Sci. Numer. Simul.*, vol. 17, no. 6, pp. 2602–2608, Jun. 2012.

[18] S. P. Bhat and D. S. Bernstein, "Finite-time stability of continuous autonomous systems," *SIAM J. Control Optim.*, vol. 38, no. 3, pp. 751–766, Jan. 2000.

[19] X. Xi, S. Mobayen, H. Ren, and S. Jafari, "Robust finite-time synchronization of a class of chaotic systems via adaptive global sliding mode control," *J. Vib. Control*, vol. 24, no. 17, pp. 3842–3854, Sep. 2018.

[20] T. Sangpet and S. Kuntanapreeda, "Finite-time synchronization of hyperchaotic systems based on feedback passivation," *Chaos, Solitons Fractals*, vol. 132, Mar. 2020, Art. no. 109605.

[21] M. Pourmahmood Aghababa and H. Pourmahmood Aghababa, "Adaptive finite-time synchronization of non-autonomous chaotic systems with uncertainty," *J. Comput. Nonlinear Dyn.*, vol. 8, no. 3, Jul. 2013, Art. no. 031006.

[22] J. Sun, Y. Shen, X. Wang, and J. Chen, "Finite-time combination-combination synchronization of four different chaotic systems with unknown parameters via sliding mode control," *Nonlinear Dyn.*, vol. 76, no. 1, pp. 383–397, Apr. 2014.

[23] H.-Y. Li, Y.-A. Hu, and R.-Q. Wang, "Adaptive finite-time synchronization of cross-strict feedback hyperchaotic systems with parameter uncertainties," *Kybernetika*, vol. 49, no. 4, pp. 554–567, 2013.

[24] J. Wang, T. Gao, and G. Zhang, "Adaptive finite-time control for hyperchaotic Lorenz–Stenflo systems," *Phys. Scr.*, vol. 90, no. 2, p. 25204, 2015.

[25] D. Zhang, J. Mei, and P. Miao, "Global finite-time synchronization of different dimensional chaotic systems," *Appl. Math. Model.*, vol. 48, pp. 303–315, Aug. 2017.

[26] Z. Sun, W. Zhu, G. Si, Y. Ge, and Y. Zhang, "Adaptive synchronization design for uncertain chaotic systems in the presence of unknown system parameters: A revisit," *Nonlinear Dyn.*, vol. 72, no. 4, pp. 729–749, Jun. 2013.

[27] H. Wang, Z.-Z. Han, Q.-Y. Xie, and W. Zhang, "Finite-time synchronization of uncertain unified chaotic systems based on CLF," *Nonlinear Anal., Real World Appl.*, vol. 10, no. 5, pp. 2842–2849, Oct. 2009.
[28] Y. Shtessel, C. Edwards, L. Fridman, and A. Levant, *Sliding Mode Control and Observation*. New York, NY, USA: Birkhauser, 2014.
[29] S. Yu, X. Yu, B. Shirinzadeh, and Z. Man, "Continuous finite-time control for robotic manipulators with terminal sliding mode," *Automatica*, vol. 41, no. 11, pp. 1957–1964, Nov. 2005.
[30] S. Laghrouche, J. Liu, F. S. Ahmed, M. Harmouche, and M. Wack, "Adaptive second-order sliding mode observer-based fault reconstruction for PEM fuel cell air-feed system," *IEEE Trans. Control Syst. Technol.*, vol. 23, no. 3, pp. 1098–1109, May 2015.
[31] A. Chen, J. Lu, J. Lu, and S. Yu, "Generating hyperchaotic Lü attractor via state feedback control," *Phys. A, Stat. Mech. Appl.*, vol. 364, pp. 103–110, May 2006.
[32] X. Wang and M. Wang, "A hyperchaos generated from Lorenz system," *Phys. A, Stat. Mech. Appl.*, vol. 387, no. 14, pp. 3751–3758, Jun. 2008.
[33] J. P. Singh and B. K. Roy, "Simplest hyperchaotic system with only one piecewise linear term," *Electron. Lett.*, vol. 55, no. 7, pp. 378–380, Apr. 2019.
[34] P. Prakash, K. Rajagopal, I. Koyuncu, J. P. Singh, M. Alcin, B. K. Roy, and M. Tuna, "A novel simple 4-D hyperchaotic system with a saddle-point Index-2 equilibrium point and multistability: Design and FPGA-based applications," *Circuits, Syst., Signal Process.*, vol. 39, no. 9, pp. 4259–4280, Sep. 2020.
[35] H. Jahanshahi, A. Yousefpour, Z. Wei, R. Alcaraz, and S. Bekiros, "A financial hyperchaotic system with coexisting attractors: Dynamic investigation, entropy analysis, control and synchronization," *Chaos, Solitons Fractals*, vol. 126, pp. 66–77, Sep. 2019.
[36] Q. Yang and C. Chen, "A 5D hyperchaotic system with three positive Lyapunov exponents coined," *Int. J. Bifurcation Chaos*, vol. 23, no. 6, Jun. 2013, Art. no. 1350109.
[37] D. Ginoya, P. D. Shendge, and S. B. Phadke, "Sliding mode control for mismatched uncertain systems using an extended disturbance observer," *IEEE Trans. Ind. Electron.*, vol. 61, no. 4, pp. 1983–1992, Apr. 2014.
[38] J. Mendoza-Avila, J. A. Moreno, and L. Fridman, "Continuous twisting algorithm for third order systems," *IEEE Trans. Autom. Control*, early access, Aug. 1, 2019, doi: 10.1109/TAC.2019.2932690.
[39] M. M. Al-Sawalha and M. S. M. Noorani, "Anti-synchronization of two hyperchaotic systems via nonlinear control," *Commun. Nonlinear Sci. Numer. Simul.*, vol. 14, no. 8, pp. 3402–3411, Aug. 2009.
[40] A. N. Njah, "Tracking control and synchronization of the new hyperchaotic Liu system via backstepping techniques," *Nonlinear Dyn.*, vol. 61, nos. 1–2, pp. 1–9, Jul. 2010.
[41] Q. Jia, "Projective synchronization of a new hyperchaotic Lorenz system," *Phys. Lett. A*, vol. 370, no. 1, pp. 40–45, Oct. 2007.
[42] H. Du, Q. Zeng, and C. Wang, "Function projective synchronization of different chaotic systems with uncertain parameters," *Phys. Lett. A, Gen. At. Solid State Phys.*, vol. 372, no. 33, pp. 5402–5410, Aug. 2008.
[43] J. Luo, S. Qu, Z. Xiong, E. Appiagyei, and L. Zhao, "Observer-based finite-time modified projective synchronization of multiple uncertain chaotic systems and applications to secure communication using DNA encoding," *IEEE Access*, vol. 7, pp. 65527–65543, 2019.
[44] A. Polyakov, "Nonlinear feedback design for fixed-time stabilization of linear control systems," *IEEE Trans. Autom. Control*, vol. 57, no. 8, pp. 2106–2110, Aug. 2012.
[45] J. A. Moreno and M. Osorio, "A Lyapunov approach to second-order sliding mode controllers and observers," in *Proc. IEEE Conf. Decis. Control*, Dec. 2008, pp. 2856–2861.
[46] A. Polyakov and L. Fridman, "Stability notions and Lyapunov functions for sliding mode control systems," *J. Franklin Inst.*, vol. 351, no. 4, pp. 1831–1865, Apr. 2014.
[47] V. I. Utkin, *Sliding Modes Control Optimization*. Berlin, Germany: Springer-Verlag, 2013.
[48] H. K. Khalil and J. W. Grizzle, *Nonlinear Systems*, vol. 3. Upper Saddle River, NJ, USA: Prentice-Hall, 2002.
[49] M. Zhihong, A. P. Paplinski, and H. R. Wu, "A robust MIMO terminal sliding mode control scheme for rigid robotic manipulators," *IEEE Trans. Autom. Control*, vol. 39, no. 12, pp. 2464–2469, Dec. 1994.
[50] X. Yu and M. Zhihong, "Fast terminal sliding-mode control design for nonlinear dynamical systems," *IEEE Trans. Circuits Syst. I, Fundam. Theory Appl.*, vol. 49, no. 2, pp. 261–264, Feb. 2002.
[51] A. Modiri and S. Mobayen, "Adaptive terminal sliding mode control scheme for synchronization of fractional-order uncertain chaotic systems," *ISA Trans.*, to be published, doi: 10.1016/j.isatra.2020.05.039.
[52] Z.-P. Jiang, "A note on chaotic secure communication systems," *IEEE Trans. Circuits Syst. I, Fundam. Theory Appl.*, vol. 49, no. 1, pp. 92–96, Jan. 2002.

XUAN-TOA TRAN received the B.S. degree in control theory from the Hanoi University of Science and Technology, Hanoi, Vietnam, in 2009, and the Ph.D. degree in control engineering from the University of Ulsan, South Korea, in 2016.

He is currently a Postdoctoral Associate with the School of Mechanical, Aerospace and Nuclear Engineering, Ulsan National Institute of Science and Technology (UNIST), Ulsan, South Korea. His research interests include nonlinear control theory, robust adaptive control, and the control for chaotic systems, robotics, and unmanned aircraft, particularly, via sliding mode control, finite-time control/observer, and adaptive finite-time control.

CHEOLHYEON KWON (Member, IEEE) received the B.S. degree in mechanical and aerospace engineering from Seoul National University, Seoul, South Korea, in 2010, and the M.S. and Ph.D. degrees from the School of Aeronautics and Astronautics, Purdue University, West Lafayette, IN, USA, in 2013 and 2017, respectively. He is currently an Assistant Professor with the School of Mechanical, Aerospace and Nuclear Engineering, Ulsan National Institute of Science and Technology (UNIST), Ulsan, South Korea. His research interests include control and estimation for dynamical cyber-physical systems (CPS), along with networked autonomous vehicles, air traffic control systems, sensors, and communication networks. His recent work aims at the cyber secure and high-assurance CPS design, inspired by control and estimation theory perspective, with applications to aerospace systems, such as unmanned aircraft systems (UAS).

HYONDONG OH (Senior Member, IEEE) received the B.Sc. and M.Sc. degrees in aerospace engineering from the Korea Advanced Institute of Science and Technology (KAIST), South Korea, in 2004 and 2010, respectively, and the Ph.D. degree in autonomous surveillance and target tracking guidance using multiple UAVs from Cranfield University, U.K., in 2013. He worked as a Lecturer in autonomous unmanned vehicles at Loughborough University, U.K., from 2014 to 2016. He is currently an Associate Professor with the School of Mechanical, Aerospace and Nuclear Engineering, Ulsan National Institute of Science and Technology (UNIST), South Korea. His research interests include autonomy and decision making, cooperative control and path planning, nonlinear guidance and control, and estimation and sensor/information fusion for unmanned systems.